Optical Photometry of the Dwarf Nova QZ Serpentis in Outburst

Frank A. Kahle
Hilden, Germany; fakahle@web.de

Received April 21, 2020; revised September 8, 2020; accepted September 9, 2020

Abstract We present white-light and two-colour photometry of the dwarf nova QZ Serpentis during the 2020 March outburst and performed differential photometry in the filters Clear (white-light), Johnson–Cousins V and Johnson–Cousins R with respect to the comparison star USNOB1.0 1112-0250654. All observations were obtained in Hilden (Germany). A radial velocity study by Thorstensen *et al.* (2017) shows this system has an orbital period of 119.75 minutes. After removing linear trends in our data we estimate a superhump period of $P_{sh} = 0.0855537 \pm 0.0000421$ days and a mass ratio of $q = 0.133 \pm 0.012$.

1. Introduction

QZ Serpentis belongs to the class of dwarf novae, close binaries with a late-type main sequence secondary star filling its Roche lobe, transferring material through the inner Langrangian point L1 to the primary star. This transfer of material forms an accretion disk around the white dwarf primary star. These objects exhibit interesting effects due to the presence of an accretion disk, and various theories exist to explain these effects observed in dwarf novae. Theories such as change in mass-transfer rate (Bath 1973) and disk instability (Osaki 1974) offer explanations for effects observed when studying dwarf novae. These binary systems are known to have periods of quiescence, outbursts, and superoutbursts (Warner 1995).

The dwarf nova QZ Ser was discovered in 1998 by Katsumi Haseda. QZ Ser is located at J2000 R. A. $15^h\ 56^m\ 54.47^s$, Dec. +21° 07' 19.0". Thorstensen *et al.* (2017) report the ephemeris $T_0 = 52438.8144$ and $P = 0.08316078$ day for the orbital period. From Thorstensen *et al.* (2002) we find the magnitude of the secondary star as $V = 17.9 \pm 0.4$. For a finder chart see Figure 1.

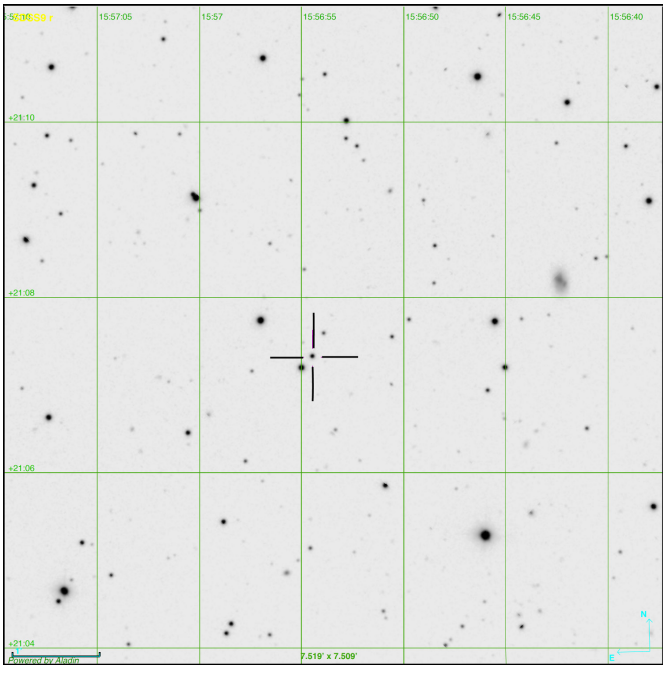

Figure 1. Finder chart for QZ Ser from "Aladin Sky Atlas." Note the V = 16.019 mag star app. 6" SE of QZ Ser.

In this paper, we present optical photometry of QZ Ser in the filters Clear (white-light), Johnson V, and Cousins R. The majority of the data were collected using the Clear filter.

2. Observations

From Schmeer (2020) we found QZ Ser to be in outburst on 2020 March 20. Our observations began two days later on 2020 March 21/22 in Hilden, Germany, using a 23.5-cm f/10 Celestron Schmidt-Cassegrain type telescope equipped with a f/6.3 focal reducer and a Moravian G2-1600 CCD camera (KAF-1603ME) operated in 2 × 2-binning. The scale of the camera was 2.44"/pixel, providing a 31.3' × 20.86' field of view.

We followed the outburst for roughly three weeks and collected data on fourteen nights. The complete list of observations is shown in Table 1. A typical image sequence consists of sets of 5 × C, R, V, R, 5 × C images and in total we collected 1,880 C (Clear) frames, 277 V frames, and 376 R frames. The Clear-band (white-light) exposure times have been set to 60 secs except for JD 2458951, where the Clear-band exposure times have been set to 70 seconds.

On each night we observed at least one full orbital period of QZ Ser. All Julian Dates reported in this paper have been heliocentrically corrected (HJD). The QZ Ser observations from HJD 2458947 and HJD 2458949 were acquired during full moon with approximately 47° and 38° separation, respectively, between QZ Ser and the moon.

3. Data reduction

The images were calibrated using standard IRAF and PYRAF software (IRAF (Tody 1986) is distributed by the National Optical Astronomy Observatories, which are operated by the Association of Universities for Research in Astronomy, Inc., under cooperative agreement with the National Science Foundation; PYRAF is a product of the Space Telescope Science Institute, which is operated by AURA for NASA). Bias frames, darks frames, and flat fields were median combined to create master frames using IRAF. Images were bias subtracted, dark subtracted, and flat divided. The CCD was kept at –10° C for all exposures. Each image was plate-solved with the Astrometry.net software package (Lang *et al.* 2010).

Table 1. Observation log.

UT date (yyyy-mm-dd)	*Epoch (JD hel.) 2450000+*	*Seeing (arcsec)*	*Filter*	*#*	*Remark*
2020-03-21/22	8930	1.90 ± 0.22	Clear (60s), V, R	140, C, 16, V, 28, R	
2020-03-22/23	8931	2.20 ± 0.67	V	87, V	
2020-03-23/24	8932	2.01 ± 0.25	Clear (60s), V, R	80, C, 8, V, 16, R	
2020-03-24/25	8933	1.68 ± 0.22	Clear (60s), V, R	90, C, 9, V, 18, R	
2020-03-25/26	8934	1.94 ± 0.29	Clear (60s), V, R	90, C, 9, V, 18, R	
2020-03-26/27	8935	1.54 ± 0.19	Clear (60s), V, R	90, C, 9, V, 18, R	
2020-03-27/28	8936	1.73 ± 0.20	Clear (60s), V, R	100, C, 10, V, 20, R	
2020-03-29/30	8938	2.26 ± 0.31	Clear (60s), V, R	140, C, 14, V, 28, R	
2020-03-31/01	8940	1.88 ± 0.37	Clear (60s), V, R	200, C, 20, V, 40, R	
2020-04-04/05	8944	1.98 ± 0.26	Clear (60s), V, R	200, C, 20, V, 40, R	
2020-04-05/06	8945	1.57 ± 0.19	Clear (60s), V, R	190, C, 19, V, 38, R	
2020-04-07/08	8947	1.66 ± 0.17	Clear (60s), V, R	190, C, 19, V, 38, R	full moon
2020-04-09/10	8949	1.60 ± 0.22	Clear (60s), V, R	200, C, 20, V, 40, R	full moon
2020-04-11/12	8951	1.66 ± 0.17	Clear (70s), V, R	170, C, 17, V, 34, R	Clouds

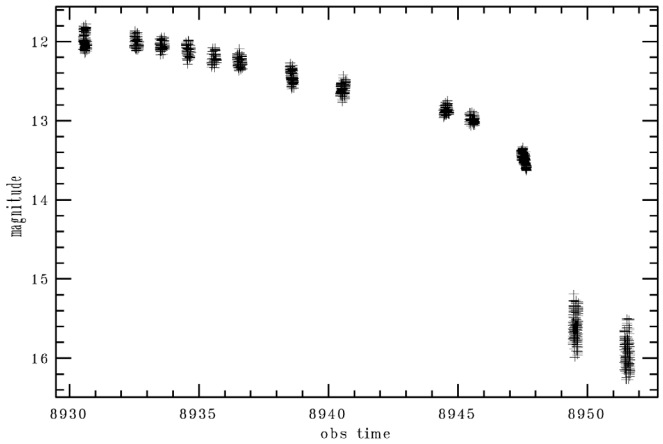

Figure 2. Clear-band light curve of QZ Ser from point-spread-function photometry during March 2020 superoutburst. The magnitude zero point for Clear and V-band are both set to 13.154 for the comparison star USNOB1.0 1111-0250033.

QZ Ser and several other stars were measured on each frame using the aperture photometry task phot from the IRAF implementation of DAOphot, with aperture radius set to 15". We note that our aperture photometry of QZ Ser is contaminated by the close neighbor USNOB1.0 1111-0250033. This star is approximately 6" SE of QZ Ser and has magnitude V = 16.019 (Zacharias *et al.* 2015). Because of the large magnitude difference this close neighbor does not affect our aperture photometry during outburst but it provides a significant flux contribution to our aperture photometry after QZ Ser has entered the dip phase. Therefore we switched to point spread function photometry whenever the close neighbor provided a significant flux contribution to our aperture photometry of QZ Ser.

We chose USNOB1.0 1112-0250654 (J2000 R.A. 15^h $57^m10.1^s$, Dec. +21° 13' 29.86"), alias 000-BBW-766 from AAVSO Chart X25228XE, as the comparison star to perform differential photometry. From AAVSO Chart X25228XE we find the comparison star V magnitude 13.253 ± 0.021. Lacking a comparison star R magnitude we estimated the comparison star's R magnitude using the transformations between SDSS and Johnson-Cousins Photometry from Jordi *et al.* (2006).

From APASS (Henden 2019) we find the magnitudes Johnson V = 13.154 ± 0.084, Sloan g = 13.461 ± 0.137, Sloan r = 13.046 ± 0.026, and Sloan i = 12.935 ± 0.037 for the comparison star. From the transformation g–r = (1.646 ± 0.008) (V–R) – (0.139 ± 0.004) we estimate R = 12.817 mag.

Since we calculated the comparison star R magnitude from APASS Sloan magnitudes we will make use of the comparison star APASS V magnitude instead of the V magnitude from AAVSO Chart X25228XE. Hereinafter 13.154 and 12.817 will be used as the comparison star V and R magnitudes.

Finally we note that no color correction has been applied to our V and R measurements.

4. Discussion

Figure 2 shows the overall light curve of QZ Ser by our CCD photometry during the 2020 March superoutburst. Since QZ Ser was reported to be in outburst on March 20 (Schmeer 2020) we may conclude that the outburst lasted at least 20 days and from Kato (2020a) we remark that superhumps were clearly present on March 21. Our light curve obtained on March 22/23 (Figure 4a) shows superhumps with an amplitude of 0.275 mag. Observational evidence for the onset of the dip after the plateau phase is clearly visible at approximately JD 2458947 from Figure 2.

From IRAF task polyfit we estimate that QZ Ser was fading in white light at a rate of 0.07(4) mag per day during the plateau phase (see Table 2 for fading rates in all three filters C, V, and R). To search for periodic signals in the light curve we used IRAF task pdm, and the generalized Lomb-Scargle (LS) and Analysis of Variance (AoV) period search implementations in the software package VARTOOLS (Hartman and Bakos 2016). After removing the linear trend of decline in our data obtained during the plateau phase we find the period candidate $P_{pdm} = 0.0855735764$ day with IRAF task pdm, whereas from the vartools search methods the candidates $P_{LS} = 0.08558217$ day and $P_{AoV} = 0.08550537$ day were found for the superhump period. Our first two nights of observations have been excluded from this calculation to avoid the inclusion of stage A superhumps. Combining these results we estimate a superhump period P_{sh} 0.0855537 ± 0.0000421 day.

Table 2. Fading rates.

Filter	*Fading mag/day*	*Remark*
Clear	0.07(4)	2458932 ≤ JD < 2458946 (1,120 obs.)
V	0.07(2)	2458932 ≤ JD < 2458946 (110 obs.)
R	0.07(0)	2458932 ≤ JD < 2458946 (216 obs.)

Table 3. Times of maximum light of QZ Ser.

Max JD hel. 2450000+	*Error*	*Filter*	*E[a] #*	*O–C[a] (days)*
8930.56438	0.0014	Clear	–23	–0.01488
8930.64994	0.0014	Clear	–22	–0.01491
8931.59103	0.0014	V	–11	–0.00382
8932.53212	0.0014	Clear	0	0
8932.61767	0.0014	Clear	1	0.00343
8933.55875	0.0014	Clear	12	0.01279
8934.49986	0.0028	Clear	23	0.01997
8934.58541	0.0028	Clear	24	0.00973
8935.61205	0.0014	Clear	36	0.01793
8936.46759	0.0014	Clear	46	0.02311
8936.55314	0.0014	Clear	47	0.02323
8936.63870	0.0014	Clear	48	0.02289
8938.52088	0.0014	Clear	70	0.01590
8938.60643	0.0014	Clear	71	0.00907
8940.48861	0.0014	Clear	93	0.01669
8940.57417	0.0014	Clear	94	0.01514
8940.65972	0.0014	Clear	95	0.00956
8944.50964	0.0014	Clear	140	0.01341
8944.59519	0.0014	Clear	141	0.00510
8945.45073	0.0014	Clear	151	0.01065
8945.53628	0.0014	Clear	152	0.01303
8945.62184	0.0014	Clear	153	0.01298
8947.50402	0.0014	Clear	175	0.00816
8949.47175	0.0014	Clear	198	0.01087
8949.55731	0.0014	Clear	199	0.01033
8951.43949	0.0014	Clear	221	0.01142
8951.52504	0.0014	Clear	222	0.00821
8951.61060	0.0014	Clear	223	0.00974

[a] *Against max = 2458932.53212 + 0.0855537 E.*

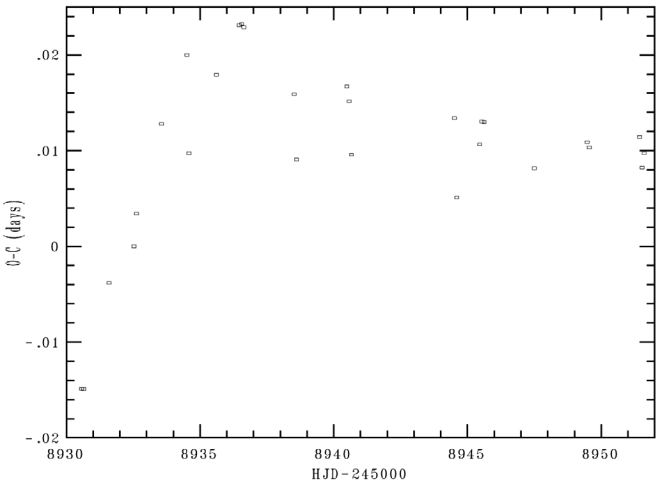

Figure 3. O–C diagram of superhump maxima of QZ Ser during the superoutburst. An ephemeris of HJD = 2458932.53212 + 0.0855537 E was used to draw this figure.

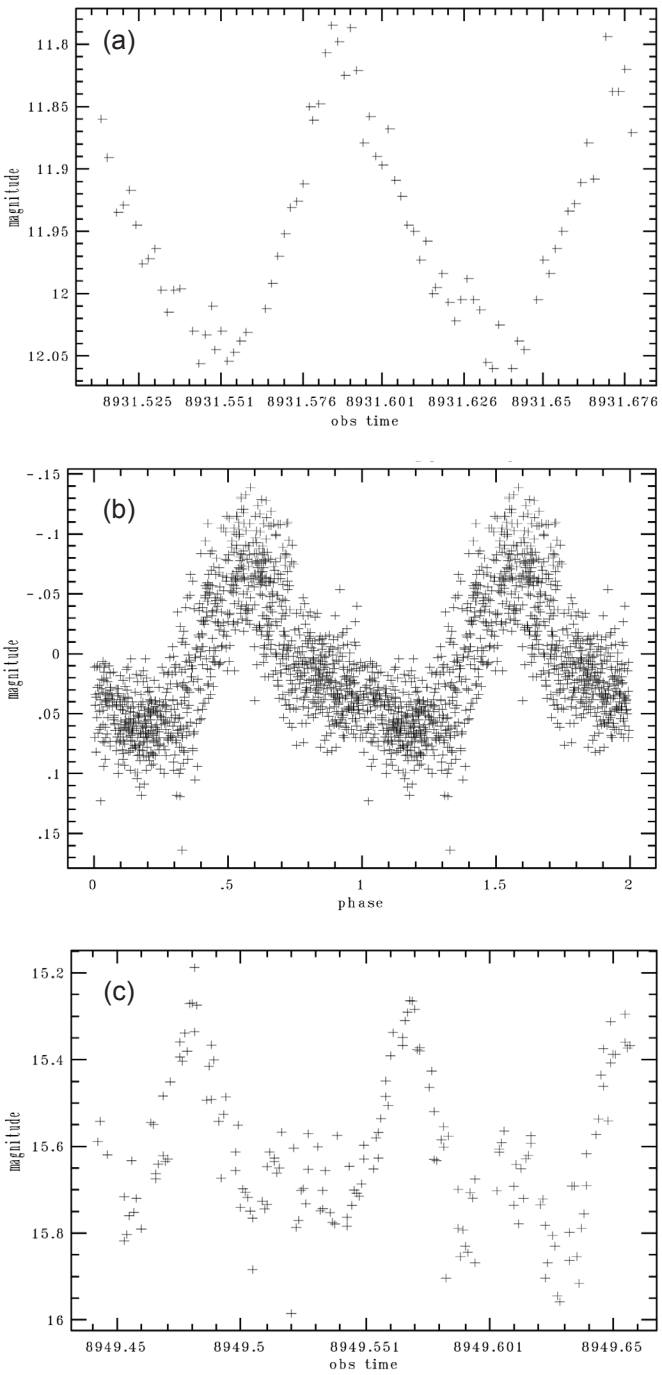

Figure 4. (a) V-band light curve for JD 2458931. (b) Detrended and phased Clear-band light curve during plateau phase. (c) Clear-band light curve for JD 2458949 from psf photometry.

The times of superhump maxima and the coresponding O–C diagram are shown in Table 3 and Figure 3. The times of maximum light have been derived from a cubic fit around each maximum. From Figure 3 we expect the transition from Stage A to Stage B superhumps approximately at HJD 2458934 / 35.

5. Acknowledgements

This research made use of the NASA Astrophysics Data System.

We are grateful to numerous collaborators of VSNET (Kato *et al.* 2004), including participants of CVNET and BAA,VSS alert, for the large contribution and to outburst detection and announcement by a number of variable star observers worldwide. We gratefully acknowledge the VSNET email notification service and the useful comments from an anonymous referee. We thank all contributors to the IRAF Community Distribution made available on github (https://iraf-community.github.io.) after NOAO dropped support for IRAF.

This research has made use of "Aladin sky atlas" (Bonnarel *et al.* 2000) developed at CDS, Strasbourg Observatory, France.

References

Bath, G. T. 1973, *Nat. Phys. Sci.*, **246**, 84.

Bonnarel, F., *et al.* 2000, *Astron. Astrophys., Suppl. Ser.*, **143**, 33.

Hartman, J. D., and Bakos, G. Á. 2016, *Astron. Comput.*, **17**, 1.

Henden, A. A. 2019, *J. Amer. Assoc. Var. Star Obs.*, **47**, 130.

Jordi, K., Grebel, E. K., and Ammon, K. 2006, *Astron. Astrophys.*, **460**, 339.

Kato, T. 2020a, vsnet-outburst 24846 (http://ooruri.kusastro.kyoto-u.ac.jp/mailarchive/vsnet-outburst/24846).

Kato, T. 2020b, vsnet-campaign-dn 9426 (http://ooruri.kusastro.kyoto-u.ac.jp/mailarchive/vsnet-campaign-dn/9426).

Kato, T., Uemura, M., Ishioka, R., Nogami, D., Kunjaya, C., Baba, H., and Yamaoka, H. 2004, *Publ. Astron. Soc. Japan*, 56, S1.

Lang, D., Hogg, D. W., Mierle, K., Blanton, M., and Roweis, S. 2010, *Astron. J.*, **139**, 1782.

Osaki, Y. 1974, *Publ. Astron. Soc. Japan*, **26**, 429.

Patterson, J. 2001, *Publ. Astron. Soc. Pacific*, **113**, 736.

Schmeer, P. 2020, vsnet-alert 24084 (http://ooruri.kusastro.kyoto-u.ac.jp/mailarchive/vsnet-alert/24084).

Thorstensen, J. R., Fenton, W. H., Patterson, J., Kemp, J., Halpern, J., and Baraffe, I. 2002, *Publ. Astron. Soc. Pacific*, **114**, 1117.

Thorstensen, J. R., Ringwald, F. A., Taylor, C. J., Sheets, H. A., Peters, C. S., Skinner, J. N., Alper, E. H., and Weil, K. E. 2017, *Res. Notes Amer. Astron. Soc.*, **1**, 29.

Tody, D. 1986, in *Instrumentation in Astronomy*, Society of Photo-Optical Instrumentation Engineers, Bellingham, Wash., 733.

Warner, B. 1995, *Cataclysmic Variable Stars*, Cambridge Univ. P., Cambridge.

Zacharias, N., *et al.* 2015, *Astron. J.*, **150**, 101.